Clinical and Immunological Features of Human BCL10 Deficiency

Blanca Garcia Solis
IdiPAZ Institute for Health Research
Ana Van Den Rym
IdiPAZ Institute for Health Research
Jareb J. Pérez-Caraballo
Vanderbilt University Medical Center
Abdulwahab Al –Ayoubi
King Saud Medical City Children's Hospital
Lazaro Lorenzo
Institut National de la Santé et de la Recherche Médicale
Carolina Cubillos-Zapata
IdiPAZ Institute for Health Research
Eduardo López-Collazo
IdiPAZ Institute for Health Research
Janet Markle
Vanderbilt University Medical Center
Miguel Fernández-Arquero
Interdepartmental Group of Immunodeficiencies
Silvia Sanchez-Ramon
Interdepartmental Group of Immunodeficiencies
Maria J. Recio
Interdepartmental Group of Immunodeficiencies
Jean-Laurent Casanova
Institut National de la Santé et de la Recherche Médicale
Reem Mohammed
Division of Allergy & Immunology King Faisal Specialist Hospital and Research Centre
Rubén Martinez-Barricarte
Vanderbilt University Medical Center
Rebeca Perez de Diego (rebeca.perez@idipaz.es)
IdiPAZ Institute for Health Research https://orcid.org/0000-0001-8426-8765

Research Article

Keywords: Primary immunodeficiency, Combined immunodeficiency, BCL10, Autosomal recessive, Lymphoid cells, mass cytometry, computational immunology, CBM complex, next-generation sequencing.

Posted Date: August 26th, 2021

DOI: https://doi.org/10.21203/rs.3.rs-807424/v1

Abstract

The CARD-BCL10-MALT1 (CBM) complex is critical for the proper assembly of human immune responses. The clinical and immunological consequences of deficiencies in some of its components such as CARD9, CARD11, and MALT1 have been elucidated in detail. However, the scarcity of BCL10 deficient patients prevented gaining that knowledge for this genetic disease. Only two patients with BCL10 deficiency have been reported to date. Here we describe in more depth an additional patient with autosomal recessive BCL10 complete deficiency caused by a nonsense mutation that leads to a loss of expression (K63X). Using mass cytometry coupled with unsupervised clustering and machine learning computational methods, we obtained a thorough characterization of the consequences of BCL10 deficiency in different populations of leukocytes. We showed that in addition to the almost absence of memory B and T cells reported before, this patient display a reduction in NK, gdT, Tregs, and T_{FH} cells. The patient suffered from recurrent respiratory infections since early in life, and showed a family history of lethal severe infectious diseases. Fortunately, hematopoietic stem-cell transplantation (HSCT) cured her. Overall, this report highlights the importance of early genetic diagnosis for the management of BCL10 deficient patients and HSCT as the recommended treatment to cured this disease.

Introduction

Primary Immunodeficiencies (PIDs) are a heterogeneous group of diseases that are now referred to as single-gene inborn errors of immunity (IEI). The in-depth functional characterization of IEI has been instrumental in treating patients better and understanding the mechanisms of human immunity[1]. The study of IEI highlighted the critical and non-redundant roles of the CARD-BCL10-MALT1 (CBM) complex in the proper assembly of human immune response [2]. Inborn errors in the components of the CBM complex cause characteristic clinical and immunological consequences [2]. Autosomal recessive complete, deficiencies in the two adaptors Caspase recruitment domain-containing (CARD) proteins, CARD9 [3] and CARD11[2, 4] cause isolated invasive fungal infections [3, 5–28] and combined immunodeficiency (CID) respectively [2, 4]. Furthermore, bi-allelic loss-of-function (LOF) mutations in the mucosa-associated lymphoid tissue lymphoma-translocation gene 1 (MALT1) cause CID [2, 4]. Numerous patients with deficiencies in CARD9, CARD11, and MALT1 have been reported, which has allowed to define the clinical presentation, immunological consequences and best treatment approaches for these three genetic diseases.

IEI in the last member of the CBM complex, B-cell lymphoma/leukemia 10 (BCL10), has been reported in only two unrelated patients [29, 30]. The first BCL10 deficient patient was reported in 2014. He was an Amerindian boy who was born to consanguineous parents and died of combined immunodeficiency (CID). The patient had autosomal-recessive complete BCL10 deficiency, resulting in an absence of wild-type (WT) mRNA and protein. The patient experienced multiple infections and active chronic colitis. T-cell and B-cell subpopulations revealed a profound deficit of memory T and B cells, a normal response in myeloid cells and a strong impact on nuclear factor kappa-light-chain-enhancer of activated B cell (NF-κB)-mediated fibroblast function [29]. Second patient, described in 2020, has an autosomal-recessive

complete BCL10 deficiency; he is an Asian-Indian boy from India with consanguineous parents. This patient suffered severe lower respiratory tract infections and immunological studies showed hypogammagloulinemia, without lymphopenia but reduced percentages of memory B cells and reduced memory T cells [30]. Hematopoietic stem cell transplantation (HSCT) was the option proposed in the patient. The present study analyses the third unrelated patient with a BCL10 deficiency by mass cytometry with un-supervised and machine learning computational methods. The patient is a child from Saudí Arabia with a related CID phenotype and a new autosomal recessive BCL10 deficiency highlighting the non-redundant role of human BCL10.

Methods

Study approval

The experimental protocol was approved by the ethics committee of La Paz University Hospital (Madrid, Spain), and written informed consent was obtained from the family for participation in this study.

Human molecular genetics and whole-exome sequencing

Genomic DNA was extracted from whole blood with a kit (Qiagen GmbH, Hilden, Germany), according to the manufacturer's instructions. Whole-exome sequencing (WES) was performed on genomic DNA from whole blood. The libraries were sequenced on an Illumina sequencing platform (mean coverage > 80 to 100X).

WES results were validated by polymerase chain reaction (PCR)/Sanger sequencing analysis on genomic DNA from whole blood. PCR was performed with PCR Master Mix (Promega, Fitchburg, WI, USA) and the GeneAmp 9700 PCR System (Applied Biosystems, Foster City, California, USA). The following primer sequences were employed for the genomic coding region of BCL10.

Forward primers (FP): 1F, TCCTCTCCTTCTTCCCCATT; 2F, GCCTGAGCCTCCTGACTTTA; 3F, GATTTGAAATAGATTATGACGGAAA.

Reverse primers (RP): 1R, AGCTCTGCGTTTAGCGATGT; 2R, GGCTGGTCTCAAAACTCCTG; 3R, AAACAAATGATTACAGCCATTTTA.

The PCR products were purified with ExoSAP-IT PCR Product Cleanup Reagent (Applied Biosystems) and sequenced with the BigDye Terminator Cycle Sequencing Kit (Applied Biosystems). Sequencing products were purified by precipitating in 70% ethanol, and the sequences were analyzed with an ABI Prism 3700 Genetic Analyser (Applied Biosystems).

Immunoblots

Human PBMCs were isolated by Ficoll-Hypaque density gradient centrifugation (Amersham-Pharmacia-Biotech, Buckinghamshire, UK) from whole-blood samples obtained from the patient, parents, siblings, and healthy volunteers, and total cell extracts were prepared. Equal amounts of protein from each sample

were separated by SDS-PAGE and blotted onto iBlot Gel Transfer Stacks (Invitrogen, Carlsbad, California, USA). These nitrocellulose membranes were then probed with anti-BCL10 rabbit mAb (ab108328, Abcam, Cambridge, MA, USA), followed by a secondary anti-rabbit IgG-HRP linked antibody (Cell Signaling, Beverly, MA, USA). Membranes were stripped and reprobed with an antibody against GADPH (Abcam) as a loading control. Antibody binding was detected by enhanced chemiluminescence (ECL; Amersham-Pharmacia-Biotech).

Mass Cytometry

Staining and data acquisition:

$5x10^6$ peripheral blood mononuclear cells (PBMCs) were stained with Cell-ID Cisplatin-^{195}Pt (Fluidigm, South San Francisco, CA) to discriminate dead cells. PBMCs were then FcR blocked with Human TruStain FcX (Biolegend, San Diego, CA), stained with the antibody mix as shown in table S1, fixed with 1.6% paraformaldehyde, and stained with Cell-ID intercalator-Ir. Stained PBMCs were analyzed in a Helios CyTOF 3.0 (Fluidigm) following manufacturer's instructions at the Cancer and Immunology Core at Vanderbilt University. The data was exported as a Flow Cytometry Standard file (FCS) and normalized using EQ bead standards (Fluidigm) following manufacturer's protocol.

Data Analysis:

For multidimensional analysis, the data was pre-gated to remove dead cells, debris, and selection of leukocytes using FlowJo 10.7.2 (Becton, Dickinson & Company, Ashland, OR), as shown in Fig S1A. The pre-gated data was exported as an FCS file and then imported into RStudio. We used the package CATALYST [31] to arcsine transform marker intensities with a cofactor of 5 and performed subsequent analysis. Unsupervised clustering was performed using FlowSOM [32], data representation was performed using the R package ggplot2, and marker enrichment modeling (MEM) [33] was used to characterize different clusters. Manual gating was performed in FlowJo, as shown in Fig S1B. Frequencies of different populations were exported from FlowJo and analyzed using Prism 9 (GraphPad Software, San Diego, CA).

Results

Homozygous BCL10 **mutation in a patient with combined immunodeficiency**

We investigated a female patient coming from a consanguineous marriage from Saudi Arabia. She presented at one year of age with fever and bacterial pneumonia that required hospitalization. Her immune workup was suggesting of hypogammaglobulinemia and lymphocytosis (see supplementary material and Table D1 for detailed clinical history). Furthermore, she had a sister who died at 12 months of age due to a severe chest infection. These observations were compatible with a PID, and she underwent WES. WES revealed a homozygous nonsense mutation (A/T) affecting the nucleotide position g.85270779 (GRCh38.p12) of exon 2 of the gene encoding BCL10 in genomic DNA (gDNA) extracted from leukocytes (g. 85270779A > T). This mutation affects the lysine at position 63 and generates a

premature stop codon (c.187A > T, p.K63X). The mutation K63X has not been reported in public databases such as ExAC or gnomAD, suggesting that it is private for this kindred. All other family members were healthy and heterozygous for the mutation (Fig. 1A and 1B). We then assessed BCL10 expression in PBMC from the patient, healthy controls, and heterozygous carriers. No BCL10 protein was detected on PBMCs from the patient, but BCL10 was detectable in the heterozygous carrier and a healthy donor (Fig. 1C). Our results indicated that this patient has a BCL10 complete deficiency.

Overt immunological phenotype in BCL10 deficient patient

We previously reported that human BCL10 is critical for the proper development and function of hematopoietic and non-hematopoietic lineages[29]. The paucity of patients with BCL10 deficiency and the limited amount of samples obtained from these patients due to the severity of their disease hindered our capacity to survey the consequences of the absence of BCL10 in the overall composition of circulating leukocytes. Furthermore, the low number of individuals reported with deleterious heterozygous variants in BCL10 prevented us from assessing the consequences of reduced dosages of BCL10 in leukocyte development and function. The samples obtained from P3, her five healthy heterozygous carrier relatives, and the advent of mass cytometry provided the tools to tackle these issues. We performed in-depth immunophenotyping of the patient, healthy heterozygous carriers, and healthy controls using mass cytometry and a cocktail of 33 antibodies directed against surface markers designed to identify most of the common leukocyte populations as well as some rare ones (Table S2). Visualization using dimensional reduction with the t-SNE algorithm revealed marked differences in the distribution of leukocyte populations when comparing a healthy control and heterozygote carrier with the patient (Fig. 2A-C). Of the subpopulations identified by unsupervised clustering followed by manual clustering (Fig. 2A-C), mucosal-associated invariant T cells (MAIT), γδT and natural killer (NK) cells showed a reduction in the patient when compared with healthy controls and heterozygous carriers (Fig. 2D). This reduction in leukocyte subpopulations is further confirmed by manual gating (Fig. 2E and S2). Considering that the patient was 1.5 years of age at the time of blood draw and the frequencies of MAIT cells at that age range from 0 to 3% of PBMCs, we cannot conclude that the reduction observed in the patient in BCL10 dependent [34]. These results suggest that BCL10 deficiency causes changes in the leukocyte population distribution otherwise not seen in healthy individuals. Despite the frequencies of $CD4^+$, $CD8^+$, B cells, and myeloid cells in the patients fall within normal ranges when compared with healthy controls (Fig. 2D), the distribution of cells within each of these populations differs between groups suggesting a subtler difference in their subpopulations (Fig. 2A, B). To further characterize these differences, we reclustered each of these populations and performed an unbiased computational analysis.

BCL10 impairs memory B cell differentiation

BCL10 is located downstream of the B-cell receptor (BCR). Upon BCR activation, the LYN kinase phosphorylates the immunoreceptor tyrosine-based activation motifs (ITAMS). These events start a molecular cascade that culminates in the activation of PI3K and a phospholipase called PLCγ2. This

molecule mediates the formation of diglycerol (DAG) as a second messenger to activate protein kinase C, which will act on CARD11 and promote the formation of the CBM complex. The formation of the CBM complex leads to the activation of the IκB complex kinase (IKK) complex, which will result in the activation of NF-κB [2]. Unsupervised clustering in the B cells from Fig. 2 identified two major populations (Fig. 3A). The frequency of cluster 2 in the patient was severely reduced compared to healthy controls and heterozygous carriers (Fig. 3B). We used marker enrichment modelling (MEM) to study these two clusters [33]. By using machine learning, MEM identifies the markers that distinguish each population allowing for an unbiased characterization of populations in an unbiased and automatic fashion. This analysis showed that cluster 1 is characterized by the expression of IgD and CD38 and cluster 2 by CD27, CD24, and CD25 (Fig. 3C). These markers are consistent with cluster 1 corresponding to naïve B cells and cluster 2 corresponding to memory B cells [35, 36]. We confirmed this observation by manual gating and observed that the patient has barely any detectable double negative or switched memory B cells with the naïve and unswitched compartments been comparable with the healthy control and heterozygous carriers (Fig. 3D, E). Our findings and the apparently abolished class switch observed in this, and the previous patients suggest that BCR signalling is dependent on BCL10. Hence, these results show that BCL10 is essential for naïve B cells to differentiate into their respective memory subpopulations.

Reduction of memory T cells in the absence of BCL10

We and others have shown that BCL10 is critical for TCR-mediated T cell activation in humans [29]. Upon TCR activation, lymphocyte-specific tyrosine kinase phosphorylates ITAMs leading to the activation of PI3K and the phospholipase PLCγ1. As is the case for B cells, these signalling events culminate in the formation of the CBM complex, which will end in the translocation of NF-κB into the nucleus and promote cell proliferation. We studied the consequence of the defective TCR activation caused by the absence of BCL10 in the composition of the T cell compartment [2]. We subsetted the $CD4^+$ and $CD8^+$ T cells identified in Fig. 2 and analysed them individually. By unsupervised clustering of the $CD4^+$ cells, we observed three major cell populations (Fig. 4A). Population 2 and 3 were severely reduced in the patient compared to healthy controls and heterozygous carriers (Fig. 4B). MEM analysis showed that cluster 1 is characterized by CD27, CCR7, CD45A, and CD38 while cells from cluster 2 express high levels of CD27, CD45RO, CCR7, CXCR3, and CD25, and cluster 3 is characterized by CD45RO expression. This differential marker expression is compatible with cluster 1 corresponding to naïve $CD4^+$ T cells and clusters 3 and 4 with memory $CD4^+$ T cells (Fig. 4C). We studied the $CD4^+$ memory and naïve compartments by manual gating (Fig. 4D, E). This analysis showed reduced central memory (CM), effector memory (EM), and TEMRA $CD4^+$ T cell compartments with an increased naïve $CD4^+$ T cell compartment in the patient when compared to the healthy controls or heterozygous carriers. Furthermore, by manual gating, we also observed a reduction in the frequency of Tregs and T_{FH} in the patient (Fig. S2). These results suggest that BCL10 is necessary for the differentiation from naïve to memory in $CD4^+$ T cells.

Similarly, unsupervised clustering of the $CD8^+$ T cell population rendered three major clusters, two of which were almost absent in the patient compared to the healthy controls and heterozygous carriers (Fig. 5A, B). Marker characterization by MEM showed that cluster 1 expressed markers characteristic of

naïve $CD8^+$ T cells such as CD45RA, CCR7. In contrast, clusters 2 and 3 are characterized by the expression of the central memory and effector memory markers (CD45RO, CD127) [37] and or TEMRA markers (CD45RA), respectively (Fig. 5C). We studied the naïve and memory $CD8^+$ T cell compartment by manual gating. Similarly to our observations in $CD4^+$ T cells, we observed an increased naïve $CD8^+$ T cell population in the patient compared to the healthy controls or heterozygous carriers. It also revealed decreased levels of central memory, effector memory, and TEMRA $CD8^+$ T cells (Figs. 5D, E). The absence of these populations in the patient suggests that BCL10 is necessary for developing the memory $CD8^+$ T cells compartment and confirms our previous results [29, 30]. As in B cell analysis, we did not observe any difference in the samples from heterozygous carriers, suggesting that haploinsufficiency for BCL10 is immunologically silent.

Normal myeloid compartment in BCL10 deficiency

Mice studies show that BCL10 is critical for NF-κB activation in myeloid cells. This is mediated by the TLR4, TLR2, and TRL6 pathways, which are BCL10 dependent. Our previous results showed that in humans, BCL10 is redundant for NF-κB activation in these cells [29]. Nevertheless, we performed unsupervised clustering in the myeloid cluster from Fig. 2. We studied 10 clusters and observed that the frequencies of these clusters were comparable between healthy controls and heterozygous carriers with the patient (Fig. S3). By manual gating, we showed that the frequencies of non-classical monocytes, classical monocytes, intermediate monocytes, myeloid dendritic cells, and plasmacytoid dendritic cells were comparable between healthy controls, heterozygous carriers, and the patient confirming the redundant role of human BCL10 in the development of cells from the myeloid lineage.

Clinical features in BCL10 deficiency

The patient presented in this study had a clinical presentation consistent with the previous two patients [29, 30] with respect to her bacterial lung infection (supplementary note 1: case report). She had a sister who died at the age of 15 mo due to disseminated BCGitis and bacterial sepsis. She did not develop any gastrointestinal manifestations, and her clinical course was cured by HSCT.

Conclusions

In this report, we describe the clinical and immunological consequences of the third human with BCL10 deficiency.

We performed cutting-edge immunophenotyping using mass cytometry to understand the effects of BCL10 in the different circulating leukocyte populations. We also applied an unsupervised and machine learning-based computational approach that allowed us to streamline the analysis and interpretation in an unbiased and automatic manner. We confirmed the results obtained by this computational approach by performing manual gating. This pipeline can speed up the characterization of the immunological consequences of this and other IEI. Our results showed that BCL10 deficiency impairs the development of memory B, $CD4^{+,}$ and $CD8^+$ T cells and confirmed previous reports [29, 30]. Surprisingly, we observed that

unswitched B cells were intact in terms of frequency which, together with the low level of IgA and IgM in the patients, suggests that the defect observed in B cells is intrinsic to them instead of secondary to the T cell deficiency observed. Furthermore, we observed a reduction in the frequencies of NK, γδT, Tregs, and Tfh. Additional experiments are necessary to understand these results better, but our data suggest that BCL10 is critical for the development or function of these cells. Overall, our in-depth immunophenotyping confirmed what we had shown in the previous two patients with BCL10 deficiency and added additional immune cell types affected by the lack of BCL10. Interestingly, when performing in-depth immunophenotyping in the healthy heterozygous carriers we did not observe any detectable defects suggesting that BCL10 haploinsufficiency is immunologically and clinically silent. Our experimental and analytical approach shows the utility of combining mass cytometry with advanced computational methods to better characterize patients with IEI.

Similar to the patient described in this manuscript, both previously reported patients had autosomal recessive BCL10 complete deficiencies leading to a lack of BCL10 protein [29, 30]. Our previous work paved the way for the early diagnosis and treatment of P3. The discovery of P3 allowed us to survey the clinical features of human BCL10 deficiency, especially in the early stages of the disease. The first BCL10 deficient patient was reported in 2014. He was an Amerindian boy born of consanguineous parents who died due to severe infections caused by his CID (Table 1) [29]. He experienced multiple infections since the age of six months, including otitis, encephalitis of unknown etiology, oral candidiasis and diaper dermatitis with *Candida albicans* superinfection, and respiratory viral infections. At the gastrointestinal level, the patient experienced active chronic colitis, prolonged diarrhea due to *Campylobacter jejuni* infection, acute gastroenteritis due to adenovirus, and diarrhea caused by *Clostridium difficile* [29] (Table 1). The second patient, an Asian-Indian boy from India with consanguineous parents, was described in 2020 [30] (Table 1). This patient suffered from severe lower respiratory tract infections, some of them requiring hospitalization. At odds with the first BCL10 deficiency [29], the second patient had not suffered from significant gastroenteritis episodes and showed a normal gastroesophageal reflux scan [30]. HSCT was the option proposed in the patient. The patient presented in this study is the third patient with a BCL10 deficiency. As mentioned above, her presentation was consistent with the previous two patients with respect to her bacterial lung infection. She did not develop any gastrointestinal manifestations, and her clinical course was cured by HSCT (Table1).

Condensing our knowledge regarding human BCL10 deficiency, from a clinical perspective, as illustrated by the fatal outcome of the first *BCL10* deficient patient [29, 38], a fast diagnosis and treatment are essential for this kind of patient. From the diagnosis standpoint, a clinical history of respiratory infections since the first months of age should be the first suspicion since it was present in all three patients (Table 1). Furthermore, a family history of severe respiratory infection in early childhood should indicate this (and other) inherited IEI. In BCL10, all patients had a sibling who died in the first months of life due to respiratory infection (Fig. 1A) [29, 30, 38], and P3. Additional evidence to suspect a BCl10 deficiency would be the absence or severe reduction of memory B and memory T cells and the reduced levels of circulating immunoglobulins comparable to those of patients with hypogammaglobulinemia has been observed in the three patients [29, 30]. Finally, BCL10 deficiency should be confirmed by sequencing and

functionally testing the putative mutant alleles. If BCL10 deficiency is confirmed, HSTC transplantation is highly recommended as the treatment of choice. Our experience supports these guidelines since the early diagnosis of P3 allowed for the application of appropriate treatment.

Declarations

ACKNOWLEDGEMENTS

We would like to thank the patient and her family for participating in this study. Support was provided by FIS grant Ref. PI17/00543, BGS is supported by PEJD2019-PRE/BMD-16556 Predoctoral Fellowships CAM. AVDR was provided support by FIS grant Ref. PI17/00543. JJPC was funded in part by an NIH training fellowship, T32GM139800, Initiative for Maximizing Student Development at Vanderbilt. RMB was funded in part by the *CTSA award No.* UL1 TR002243 *from the National Center for Advancing Translational Sciences.*

> Funding: Support was provided by FIS grant Ref. PI17/00543, BGS is supported by PEJD2019-PRE/BMD-16556 Predoctoral Fellowships CAM. AVDR was provided support by FIS grant Ref. PI17/00543. JJPC was funded in part by an NIH training fellowship, T32GM139800, Initiative for Maximizing Student Development at Vanderbilt. RMB was funded in part by the *CTSA award No.* UL1 TR002243 *from the National Center for Advancing Translational Sciences*.

> Conflicts of interest: The authors declare that they have no conflicts of interest.

> ***Availability of data and material***: All data and material are available if are request.

> ***Code availability:*** Not applicable

> Authors' contributions:

Blanca Garcia Solis, Ana Van Den Rym and Jareb J. Pérez-Caraballo: Experiments, analysis results, editing.

Abdulwahab Al –Ayoubi: Immune cells phenotype, clinical study.

Lazaro Lorenzo: Handling of cells, DNA extraction and PBMC processing.

Carolina Cubillos-Zapata: Manuscript comments, advice and editing.

Eduardo López-Collazo: Group leader, consulting on experimental procedures.

Janet Markle: CyTOF experiments.

Miguel Fernández-Arquero ,Silvia Sánchez-Ramón and Maria José Recio: Manuscript comments, advice and editing.

Jean-Laurent Casanova: Manuscript drafting and editing.

Reem Mohammed: Physician in charge of the patient's care. Clinical study.

Rubén Martinez-Barricarte: CyTOF, manuscript drafting and editing.

Rebeca Pérez de Diego: Laboratory head, experiment design, manuscript drafting and editing. Corresponding author.

***> Ethics approval,* consent to participate and consent for publication**: The experimental protocol was approved by the ethics committee of La Paz University Hospital (Madrid, Spain), and written informed consent was obtained from the family for participation and publication in this study.

References

1. Notarangelo LD, Bacchetta R, Casanova J-L, Su HC. Human inborn errors of immunity: An expanding universe. Sci Immunol [Internet]. 2020;5:eabb1662. Available from: http://immunology.sciencemag.org/content/5/49/eabb1662.abstract.
2. Lu HY, Bauman BM, Arjunaraja S, Dorjbal B, Milner JD, Snow AL, et al. The CBM-opathies—a rapidly expanding spectrum of human inborn errors of immunity caused by mutations in the CARD11-BCL10-MALT1 complex. Front Immunol. 2018;9:2078.
3. Corvilain E, Casanova JL, Puel A. Inherited CARD9 Deficiency: Invasive Disease Caused by Ascomycete Fungi in Previously Healthy Children and Adults. J Clin Immunol. 2018;38:656–93.
4. Lu HY, Biggs CM, Blanchard-Rohner G, Fung SY, Sharma M, Turvey SE. Germline CBM-opathies: From immunodeficiency to atopy. J Allergy Clin Immunol. 2019;143:1661–73.
5. Drewniak A, Gazendam RP, Tool AT, van Houdt M, Jansen MH, van Hamme JL, et al. Invasive fungal infection and impaired neutrophil killing in human CARD9 deficiency. Blood. 2013;121:2385–92.
6. Herbst M, Gazendam R, Reimnitz D, Sawalle-Belohradsky J, Groll A, Schlegel PG, et al. Chronic Candida albicans Meningitis in a 4-Year-Old Girl with a Homozygous Mutation in the CARD9 Gene (Q295X). Pediatr Infect Dis J. 2015;34:999–1002.
7. De Bruyne M, Hoste L, Bogaert DJ, Van den Bossche L, Tavernier SJ, Parthoens E, et al. A CARD9 Founder Mutation Disrupts NF-κB Signaling by Inhibiting BCL10 and MALT1 Recruitment and Signalosome Formation. Front Immunol. 2018;9:2366.
8. Arango-Franco CA, Moncada-Vélez M, Beltrán CP, Berrío I, Mogollón C, Restrepo A, et al. Early-Onset Invasive Infection Due to Corynespora cassiicola Associated with Compound Heterozygous CARD9 Mutations in a Colombian Patient. J Clin Immunol. 2018;38:794–803.
9. Vaezi A, Fakhim H, Abtahian Z, Khodavaisy S, Geramishoar M, Alizadeh A, et al. Frequency and geographic distribution of CARD9 mutations in patients with severe fungal infections. Front Microbiol. 2018;9.
10. Wang X, Wang A, Wang X, Li R, Yu J. Cutaneous mucormycosis caused by Mucor irregularis in a patient with CARD9 deficiency. Br J Dermatol. 2019;180:213–4.

11. Quan C, Li X, Shi RF, Zhao XQ, Xu H, Wang B, et al. Recurrent fungal infections in a Chinese patient with CARD9 deficiency and a review of 48 cases. Br J Dermatol. 2018;180:1221–5.
12. Sari S, Dalgic B, Muehlenbachs A, Deleon-Carnes M, Goldsmith CS, Ekinci O, et al. Prototheca zopfii Colitis in Inherited CARD9 Deficiency. J Infect Dis. 2018;218:485–9.
13. Cetinkaya PG, Ayvaz DC, Karaatmaca B, Gocmen R, Söylemezoğlu F, Bainter W, et al. A young girl with severe cerebral fungal infection due to card 9 deficiency. Clin Immunol. 2018;191:21–6.
14. Wang X, Zhang R, Wu W, Song Y, Wan Z, Han W, et al. Impaired Specific Antifungal Immunity in CARD9-Deficient Patients with Phaeohyphomycosis. J Invest Dermatol. 2018;138:607–17.
15. Gavino C, Mellinghoff S, Cornely OA, Landekic M, Le C, Langelier M, et al. Novel bi-allelic splice mutations in CARD9 causing adult-onset Candida endophthalmitis. Mycoses. 2018;61:61–5.
16. Gavino C, Cotter A, Lichtenstein D, Lejtenyi D, Fortin C, Legault C, et al. CARD9 Deficiency and Spontaneous Central Nervous System Candidiasis: Complete Clinical Remission With GM-CSF Therapy. Clin Infect Dis. 2014;59:81–4.
17. Rieber N, Gazendam RP, Freeman AF, Hsu AP, Collar AL, Sugui JA, et al. Extrapulmonary Aspergillus infection in patients with CARD9 deficiency. JCI Insight. 2016;1:e89890.
18. Alves de Medeiros AK, Lodewick E, Bogaert DJA, Haerynck F, Van daele S, Lambrecht B, et al. Chronic and Invasive Fungal Infections in a Family with CARD9 Deficiency. J Clin Immunol. 2016;36:204–9.
19. Jones N, Garcez T, Newman W, Denning D. Endogenous Candida endophthalmitis and osteomyelitis associated with CARD9 deficiency. BMJ Case Rep. 2016;bcr2015214117.
20. Celmeli F, Oztoprak N, Turkkahraman D, Seyman D, Mutlu E, Frede N, et al. Successful granulocyte colony-stimulating factor treatment of relapsing Candida Albicans meningoencephalitis caused by CARD9 deficiency. Pediatr Infect Dis J. 2016;35:428–31.
21. Gavino C, Hamel N, Zeng J, Bin, Legault C, Guiot MC, Chankowsky J, et al. Impaired RASGRF1/ERK-mediated GM-CSF response characterizes CARD9 deficiency in French-Canadians. J Allergy Clin Immunol. 2016;137:1178–88.e7.
22. Glocker E-O, Hennigs A, Nabavi M, Schäffer AA, Woellner C, Salzer U, et al. A Homozygous CARD9 Mutation in a Family with Susceptibility to Fungal Infections. N Engl J Med. 2009;361:1727–35.
23. Lanternier F, Mahdaviani SA, Barbati E, Chaussade H, Koumar Y, Levy R, et al. Inherited CARD9 deficiency in otherwise healthy children and adults with Candida species-induced meningoencephalitis, colitis, or both. J Allergy Clin Immunol. 2015;135:1558–68.e2.
24. Lanternier F, Barbati E, Meinzer U, Liu L, Pedergnana V, Migaud M, et al. Inherited CARD9 deficiency in 2 unrelated patients with invasive exophiala infection. J Infect Dis. 2015;211:1241–50.
25. L F, C S, P C, J. B OL. J.-L. C. Primary immunodeficiencies underlying fungal infections. Curr Opin Pediatr. 2013;25:736–47.
26. Lanternier F, Pathan S, Vincent QB, Liu L, Cypowyj S, Prando C, et al. Deep dermatophytosis and inherited CARD9 deficiency. N Engl J Med. 2013;369:1704–14.

27. Wang X, Wang W, Lin Z, Wang X, Li T, Yu J, et al. CARD9 mutations linked to subcutaneous phaeohyphomycosis and T H17 cell deficiencies. J Allergy Clin Immunol. 2014;133:905–8.
28. Grumach AS, de Queiroz-Telles F, Migaud M, Lanternier F, Filho NR, Palma SMU, et al. A Homozygous CARD9 Mutation in a Brazilian Patient with Deep Dermatophytosis. J Clin Immunol. 2015;35:486–90.
29. Torres JM, Martinez-Barricarte R, Garcia-Gomez S, Mazariegos MS, Itan Y, Boisson B, et al. Inherited BCL10 deficiency impairs hematopoietic and nonhematopoietic immunity. J Clin Invest. 2014;124:5239–48.
30. Van Den Rym A, Taur P, Martinez-Barricarte R, Lorenzo L, Puel A, Gonzalez-Navarro P, et al. Human BCL10 Deficiency due to Homozygosity for a Rare Allele. J Clin Immunol Netherlands. 2020;40:388–98.
31. Nowicka M, Krieg C, Crowell H, Weber L, Hartmann F, Guglietta S, et al. CyTOF workflow: differential discovery in high-throughput high-dimensional cytometry datasets. F1000Research. 2019;6:748.
32. Van Gassen S, Callebaut B, Helden M, Lambrecht B, Demeester P, Dhaene T, et al. FlowSOM: Using self-organizing maps for visualization and interpretation of cytometry data. Cytom Part A. 2015;87.
33. Diggins K, Greenplate A, Leelatian N, Wogsland C, Irish J. Characterizing cell subsets using marker enrichment modeling. Nat Methods. 2017;14:275–8.
34. Chen P, Deng W, Li D, Zeng T, Huang L, Wang Q, et al. Circulating Mucosal-Associated Invariant T Cells in a Large Cohort of Healthy Chinese Individuals From Newborn to Elderly. Front Immunol. 2019;10:260.
35. Amu S, Tarkowski A, Dörner T, Bokarewa M, Brisslert M. The Human Immunomodulatory CD25 + B Cell Population belongs to the Memory B Cell Pool. Scand J Immunol [Internet]. 2007;66:77–86. Available from: https://onlinelibrary.wiley.com/doi/abs/10.1111/j.1365-3083.2007.01946.x.
36. Wu Y-CB, Kipling D, Dunn-Walters D. The Relationship between CD27 Negative and Positive B Cell Populations in Human Peripheral Blood. Front Immunol [Internet]. 2011;2:81. Available from: https://www.frontiersin.org/article/10.3389/fimmu.2011.00081.
37. Martin MD, Badovinac VP. Defining Memory CD8 T Cell. Front Immunol [Internet]. 2018;9:2692. Available from: https://www.frontiersin.org/article/10.3389/fimmu.2018.02692.
38. Garcia-Gomez S, Alvarez Doforno R, Martinez-Barricarte R, Torres JM, Ferreira Cerdan A, Davila M, et al. Actin polymerisation after FCgammaR stimulation of human fibroblasts is BCL10 independent. Clin Immunol. 2016;163:120–2.

Tables

TABLE 1. Summary of the main genetic, clinical, immunological, and cellular features comparing the three BCL10-deficient patients reported.

	P1	P2	P3
Mutation	g.85741978C > T; IVS1+1G>A	g.85270702G>A, c.262C>T, p.R88X	g. 85270779A>T, c.187A>T, p.K63X
Zygosity	Homozygosis, consanguienous parents	Homozygosis, consanguienous parents	Homozygosis, consanguienous parents
Protein expression	No	No	No
Main Clinical Features	6mo: Gastroenteritis, otitis, and respiratory infections. 8mo: Viral infection (flu A and B, adenovirus; respiratory syncytial virus (RSV)); *acute secondary respiratory failure*, oral candidiasis, and diaper dermatitis. 13mo: Prolonged diarrhea (*Campylobacter jejuni*). 18mo: Diarrhea. Active chronic colitis. 2y 5mo: Acute gastroenteritis (adenovirus) and respiratory infection (RSV). 2y 8mo: Diarrhea (adenovirus). Chronic non-specific colitis. 2y 10mo: Seizures and *status*epilepticus. Secondary*diffuse leukoencephalopathy*. 3y 4mo: Diarrhea (*Clostridium difficile*). D*izziness, disorientation, and generalized weakness with focal abnormal movements.* Suspected encephalitis. Died due to respiratory failure.	1mo: Flare of the BCG scar with increased erythema and swelling. 6mo: Severe viral lower respiratory tract infection and palatal ulcers 8mo and 10mo: lower respiratory tract infections not requiring hospitalization 11mo: Acute onset respiratory distress (*Mycobacterium tuberculosis* was and no evidence fungal infection)	1yo: Hospitalized due to pneumonia (bacterial).
Cellular phenotype	B cells: Hypogammaglobulinemia. Lack of memory B cells.	B cells: Hypogammaglobulinemia. Deficit of memory B cells.	B cells: Hypogammaglobulinemia. Deficit of memory B cells.
	T cells: Normal total T cell number. Deficit of memory T cells. T-cell proliferation in response to TCR blocked.	T cells: Normal total T cell number. Deficit of memory T cells.	T cells: Normal total T cell number. Deficit of memory T cells.
Keys	**Suspicion:** Clinical history of respiratory infections since the first months of age. No memory lymphocytes (or reduced levels) despite normal total cell numbers, hypogammaglobulinemia. **Confirmation:***BCL10* sequencing and by measurement of BCL10 protein expression **Treatment:** HSCT		

Figures

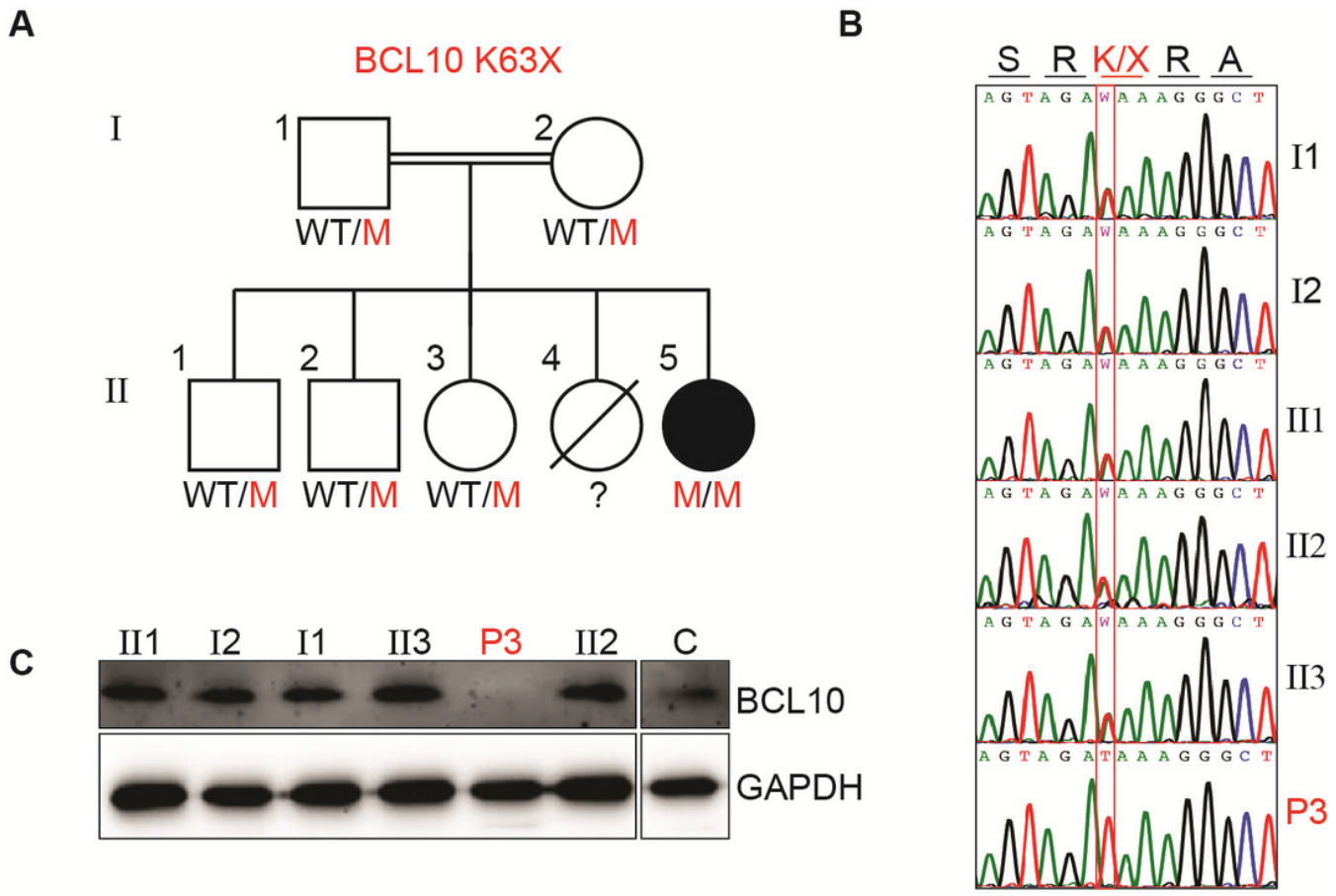

Figure 1

BCL10 deficiency in a patient with CID. (A) Familial segregation of the mutation K63X in BCL10. (B) Sanger sequencing results of P3 and her family members in the region spanning the BCL10 mutation. The amino acid consequence is indicated above the graphs. (C) Immunoblot analysis of BCL10 protein in PBMC of the patient (P3), parents (I1, I2), siblings (II1, II2, II3), and healthy control (C). GAPDH was used as a loading control. The panels illustrate the results from a single experiment, representative of three.

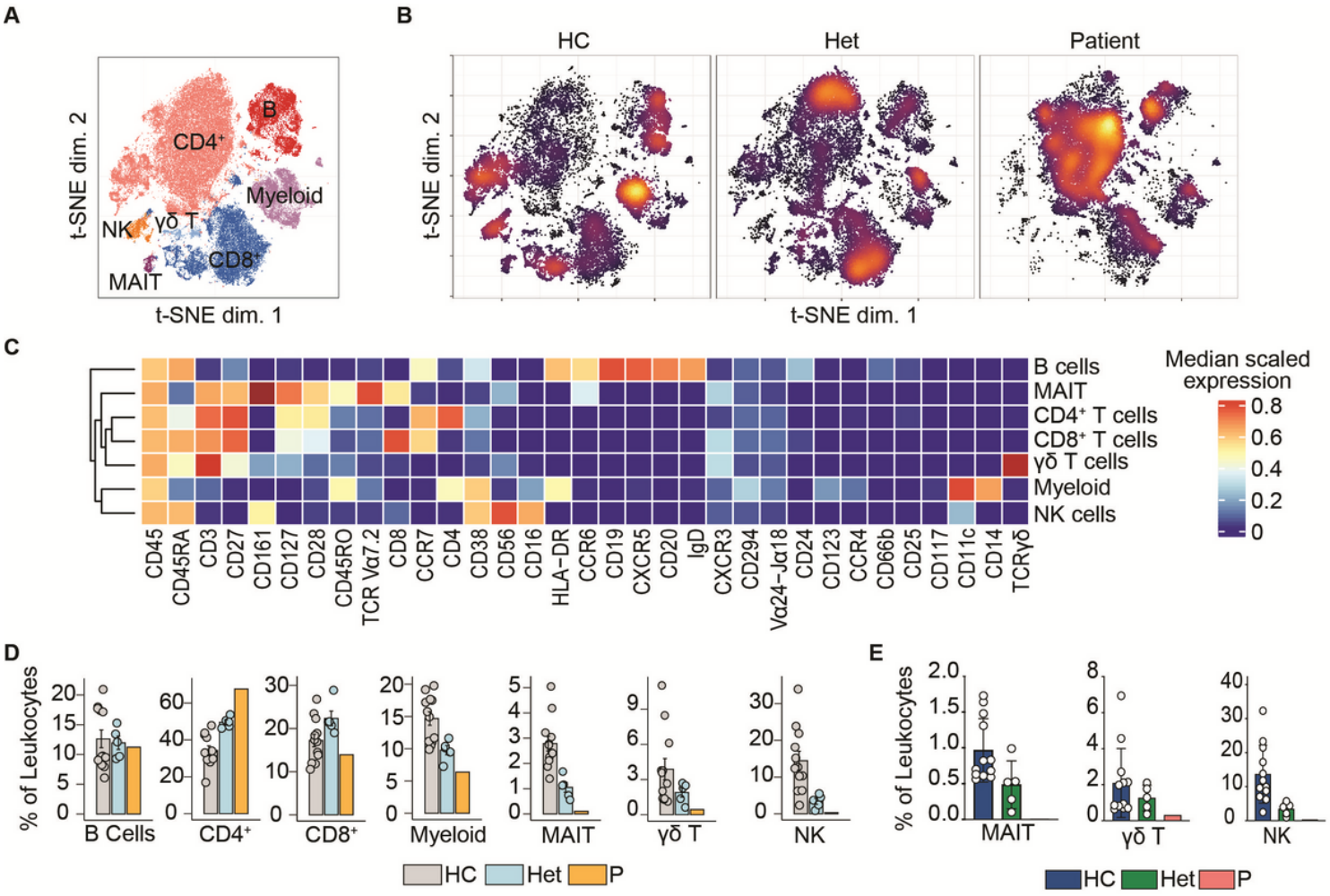

Figure 2

Leukocyte immunophenotyping. (A) Dimensional reduction by t-SNE of the 33 markers used for immunophenotyping by mass cytometry. Each color represents a cell population obtained by manual clustering according to their surface marker expression. 50,000 cells from healthy controls (HC), heterozygous carriers (Het), and the patient are represented. (B) Density t-SNE showing the distribution of leukocytes in healthy control (HC), heterozygous carrier (Het), and the patient. (C) Median expression heatmap of the markers shown under the graph, for the populations shown in A. (D) Frequencies of the populations highlighted in (A) as a percentage of leukocytes. (E) Frequencies of MAIT, γδ T, and natural killer cells in healthy controls (HC), heterozygote carrier (Het), and patient as a percentage of leukocytes obtained by manual gating in FlowJo shown in figure S2.

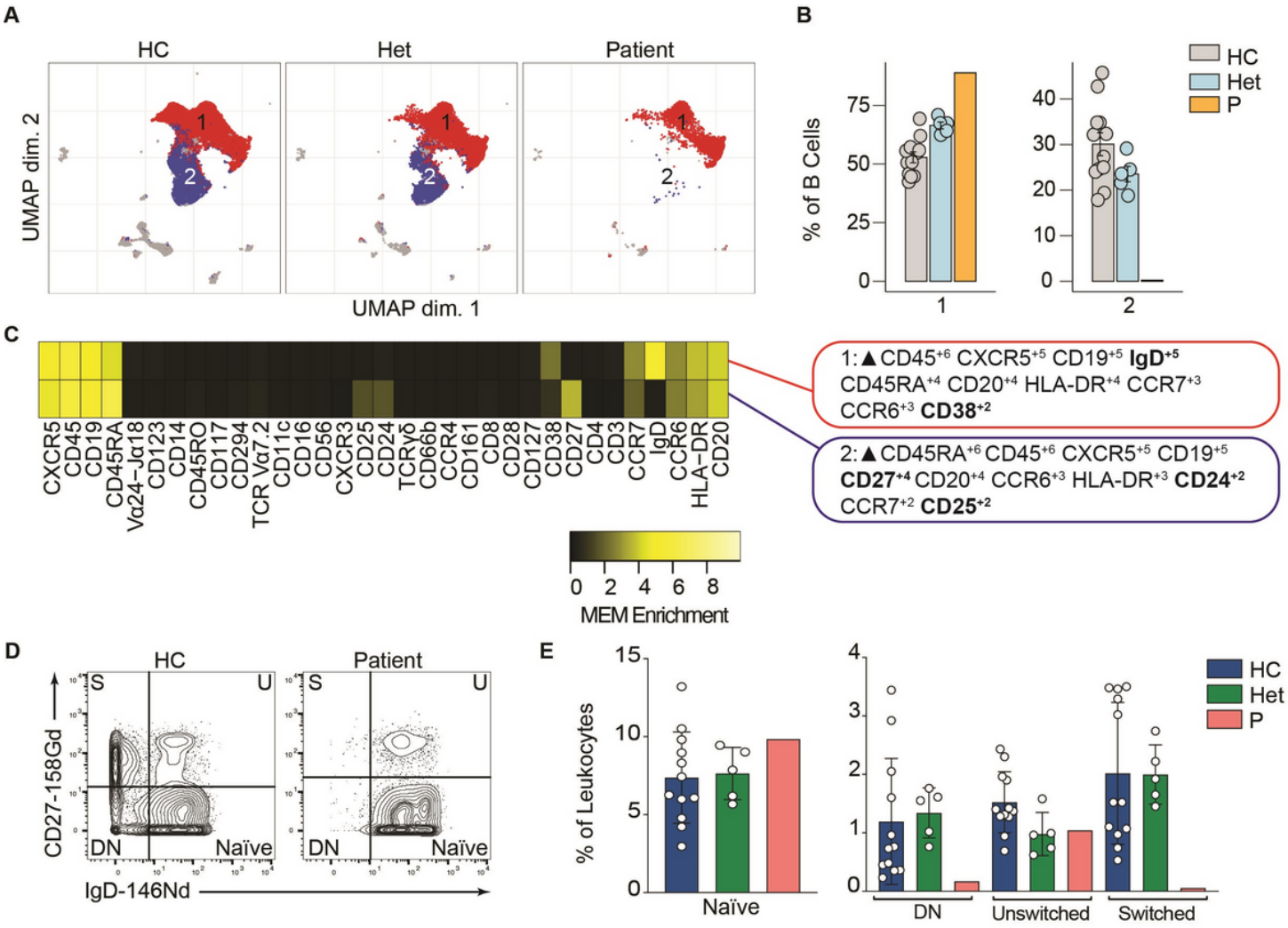

Figure 3

B cells immunophenotyping. (A) UMAP representation showing the B cell population from figure 2. Each color represents a cluster obtained by unsupervised clustering using flowSOM. 10,000 cells from healthy controls (HC), heterozygous carriers (Het), and the patient are represented. (B) Frequencies of the flowSOM clusters highlighted in (A) as a percentage of total cells in the B cell population from figure 2. (C) MEM heatmap and marker tags for the clusters shown in (A). In bold are highlighted the markers differentially expressed between clusters. (D) CD27 vs. IgD B cell manual gating example for a healthy representative control (HC) and the patient. Detailed gating strategy is shown in supplementary figure 2. (E) Frequencies of Naïve, Double Negative, switched and unswitched B cells in healthy controls (HC), heterozygote carrier (Het) and patient as a percentage of leukocytes obtained by manual gating in FlowJo.

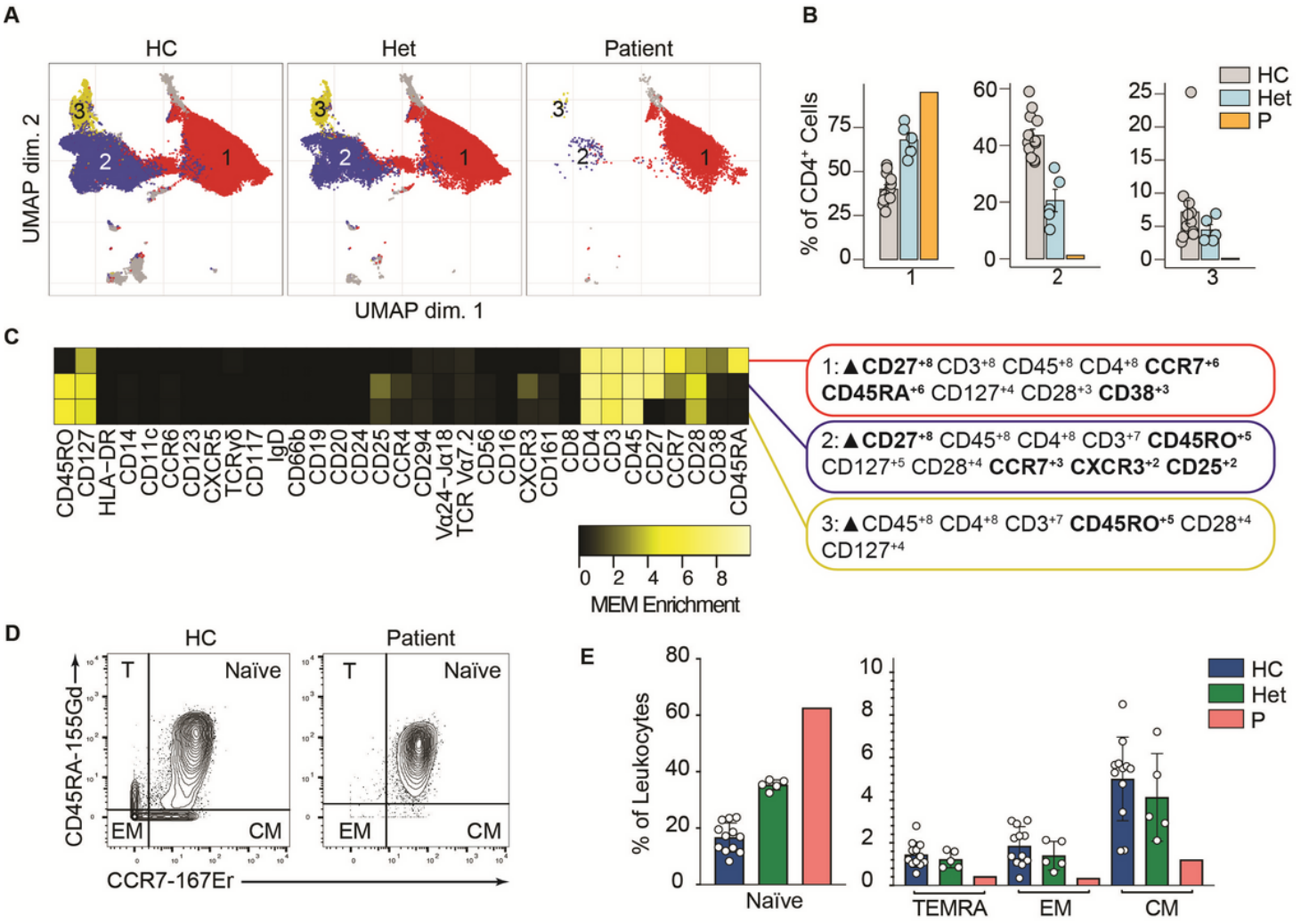

Figure 4

CD4+ T cells immunophenotyping. (A) UMAP representation showing the CD4+ T population from figure 2. Each color represents a cluster obtained by unsupervised clustering using flowSOM. 10,000 cells from healthy controls (HC), heterozygous carriers (Het), and the patient are represented. (B) Frequencies of the flowSOM clusters highlighted in (A) as a percentage of total cells in the CD4+ T cell cluster from figure 2. (C) MEM heatmap and marker tags for the clusters shown in (A). In bold are highlighted the markers differentially expressed between clusters. (D) CD45RA vs. CCR7 CD4+ T cell gating example for a representative healthy control (HC) and the patient. Detailed gating strategy is shown in supplementary figure 2. (E) Frequencies of Naïve, TEMRA, effector memory (EM) and central memory (CM) CD4+ T cells in healthy controls (HC), heterozygous carrier (Het), and patient as a percentage of leukocytes obtained by manual gating in FlowJo.

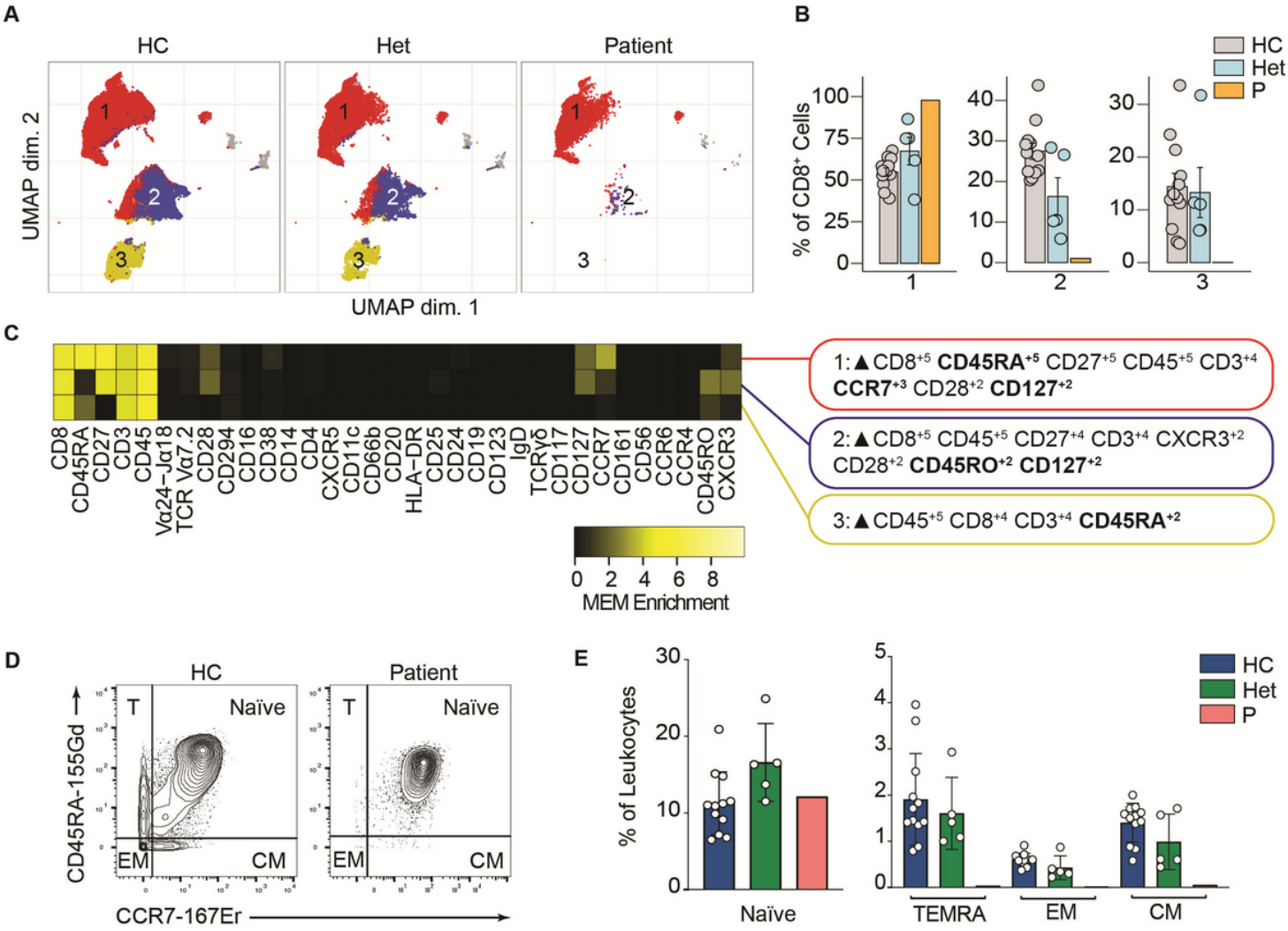

Figure 5

CD8+ T cells immunophenotyping. (A) UMAP representation showing the CD8+ T population from figure 2. Each color represents a cluster obtained by unsupervised clustering using flowSOM. 10,000 cells from healthy controls (HC), heterozygous carriers (Het) and the patient are represented. (B) Frequencies of the flowSOM clusters highlighted in (A) as a percentage of total cells in the CD8+ T cells cluster from figure 2. (C) MEM heatmap and marker tags for the clusters shown in (A). In bold are highlighted the markers differentially expressed between clusters. (D) CD45RA vs. CCR7 CD8+ cell gating example for a representative healthy control (HC) and the patient. Detailed gating strategy is shown in supplementary figure 2. (E) Frequencies of Naïve, TEMRA, effector memory (EM) and central memory (CM) CD8+ T cells in healthy controls (HC), heterozygous carrier (Het), and patient as a percentage of leukocytes obtained by manual gating in FlowJo.

Supplementary Files

This is a list of supplementary files associated with this preprint. Click to download.

- BCL10SOM.docx
- FigureS1.jpg
- FigureS2.jpg
- FigureS3.jpg
- TableS1.doc
- TableS2.doc